Biotechnology and Bioprocess Engineering 19: 747-753 (2014)
DOI 10.1007/s12257-014-0145-y

RESEARCH PAPER

Surface Modification of Cowpea Chlorotic Mottle Virus Capsids *via* a Copper(I)-catalyzed Azide-Alkyne Cycloaddition (CuAAC) Reaction and Their Adhesion Behavior with HeLa Cells

Yuanzheng Wu, Hetong Yang, Young-Jin Jeon, Min-Young Lee, Jishun Li, and Hyun-Jae Shin

Received: 28 February 2014 / Revised: 28 May 2014 / Accepted: 6 June 2014

Abstract A copper(I)-catalyzed azide-alkyne cycloaddition (CuAAC) reaction was exploited for the surface modification of cowpea chlorotic mottle virus (CCMV). The exposed carboxyl residues of the CCMV capsids were modified with an alkyne and then further modified with an azide, using a triazole connection in the presence of $CuSO_4$, tris(2-carboxyethyl)phosphine hydrochloride (TCEP), and a bathocuproin disulfonic acid disodium salt (BCDS). Fluorogenic coumarin was successfully grafted onto the CCMV capsids and monitored by fast protein liquid chromatography (FPLC) and UV-irradiated SDS-PAGE. An oligo-ethylene glycol (OEG) short chain and an Arg-Gly-Asp (RGD) peptide were also connected to the CCMV capsids *via* the CuAAC reaction. Size-exclusion FPLC, transmission electron microscopy (TEM), and dynamic light scattering (DLS) analyses confirmed the modification and integrity of the viral capsids. Interestingly, OEG-CCMV displayed a unique phenomenon of connected bridges with the intact capsids crosslinked to each other. Coumarin-CCMV, OEG-CCMV, and RGD-CCMV were absorbed onto APTES slides for cell binding with HeLa cells. The opposite adhesion behavior of OEG-CCMV and RGD-CCMV indicated the inhibition effect of OEG and the promotion effect of RGD for cell attachment. This provides a generalized method for chemical modification of the surface of virus capsids with multivalent ligands, which demonstrates the potential applications in bioimaging, tissue engineering, and drug delivery.

Keywords: CCMV, CuAAC reaction, bioconjugation, OEG, RGD, cell adhesion

Yuanzheng Wu, Hyun-Jae Shin*
Department of Chemical and Biochemical Engineering, Chosun University, Gwangju 501-759, Korea
Tel: +82-62-230-7518; Fax: +82-62-230-7226
E-mail: shinhj@chosun.ac.kr

Yuanzheng Wu, Hetong Yang, Jishun Li
Biotechnology Center of Shandong Academy of Sciences, Jinan 250-014, China

Young-Jin Jeon, Min-Young Lee
Department of Pharmacology, School of Medicine, Chosun University, Gwangju 501-759, Korea

1. Introduction

Viruses and virus-like particles (VLPs) have been employed as building blocks and templates in bionanotechnology over the last decade for their highly symmetrical structures and self-assembly properties [1,2]. Chemical and genetic manipulations on the surface of viral protein cages confer unique properties to VLPs as programmable scaffolds in bionanotechnology [3,4]. As a model plant virus, cowpea chlorotic mottle virus (CCMV) has been widely studied, and its capsid consists of 180 copies of the coat protein (CP, 20 kDa) that forms an icosahedral shell with an outer diameter of 28 nm and an inner diameter of 18 nm ($T = 3$ symmetry). The low-resolution structure of CCMV has been determined by electron cryo-microscopy (cryo-EM) at 3.2 Å [5-7]. CCMV capsids provide a versatile platform for surface modification and multivalent-ligand presentation. Most studies have focused on the constrained synthesis and encapsulation of both inorganic and organic materials, taking advantage of the structural transition of the CCMV capsids [8,9]. There are few studies on surface modification based on CCMV. As they assemble from 180 identical CP subunits, the exterior surface of CCMV capsids has multiple, highly symmetrically functional groups protruding outside

that can potentially be chemically modified for the site-specific attachment of a variety of ligands [10]. Determined by cryo-EM, each CP subunit presents up to 11 carboxylate groups (aspartic acid, D; and glutamic acid, E) exposed on the exterior surface. Similarly, there are up to 6 surface-exposed amine groups (lysine, K) per subunit [11]. This provides an estimate of up to 1980 and 1080 accessible sites for each of these functional groups, respectively, on the assembled capsid. Based on this information, Gillitzer *et al.* [12] have successfully modified the exterior surface of CCMV with both fluorescent molecules and small peptides.

There have been a variety of bioconjugation methods developed for the attachment of ligands to the exterior surfaces of virus capsids [3,13]. Among them, the copper(I)-catalyzed azide-alkyne cycloaddition (CuAAC) reaction, the most widely recognized example of click chemistry, has been rapidly embraced for applications in myriad fields since its discovery by Finn and Sharpless [14-16]. The selective reactivity between azides and alkynes (only with each other) has made this procedure tremendously attractive. Several different CuAAC variants have been reported to address specific cases involving peptides, proteins, polynucleotides, and fixed cells [17]. The CuAAC reaction provides a reliable method for coupling a wide range of molecules in a regiospecific fashion under relatively mild reaction conditions with little byproduct, which makes it a versatile and modular procedure for the modification of viral capsids. The Finn group has utilized the CuAAC reaction to conjugate both small molecules and macromolecules onto the exterior surface of the cowpea mottle virus (CPMV) and bacteriophage Qβ [18,19]. The tyrosine residues on the helical surface of tobacco mosaic virus (TMV) were coupled with chemoselective diazonium and azides *via* a sequential CuAAC reaction [20]. Various fluorescent coumarins and the Arg-Gly-Asp (RGD) peptide have also been grafted onto the surface of the turnip yellow mosaic virus (TYMV) by the CuAAC reaction [21].

In this research, we extended the CuAAC reaction to tailor CCMV capsids, following the scheme of Fig. 1. The surface-exposed amine and carboxylate residues were efficiently addressable under mild conditions. The corresponding binding studies with HeLa cells using decorated CCMV capsids presented contrasting adhesion behavior according to the various motifs introduced.

2. Materials and Methods

2.1. Materials and instruments

Unless otherwise stated, all reagents and chemicals were obtained from commercial sources and used without further purification. The molecules 7-(diethylamino)coumarin-3-carbonyl azide, oligo-ethylene glycol (OEG) bisazide, and azide-terminated RGD oligopeptide were purchased from Sigma-Aldrich or Invitrogen. The 3-aminopropyl-triethoxysilane (APTES)-functionalized slides were purchased from Labscientific. The CCMV capsids were prepared as described in the literature [21]. The purified CCMV sample (1 mg/mL) in 80% assembly buffer (100 mM sodium acetate, 1 mM EDTA, 5 mM DTT, 0.5 mM PMSF, and pH 5.2) plus 20% dimethyl sulfoxide (DMSO) was used for the process. General desalting and removal of other small molecules from the protein samples were achieved

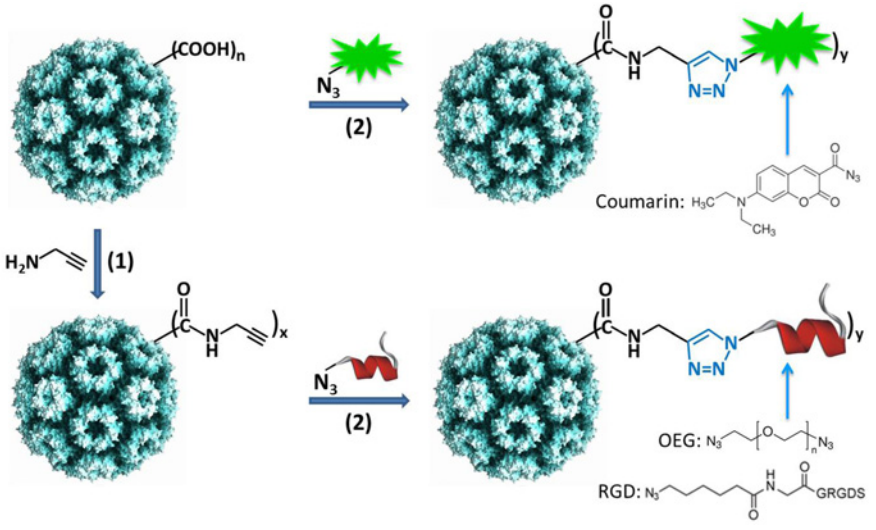

Fig. 1. Schematic diagram of bioconjugation onto CCMV capsids using the CuAAC reaction. Step (1), propargyl-amine modification to introduce alkyne motif on the exterior surface of CCMV capsids. Step (2), triazole connection of CCMV-alkyne with azide ligands of fluorescent coumarin triazole (marked in green), oligo-ethylene glycol (OEG) short chain and RGD-containing peptide (marked in red).

using centrifugal filter devices (Vivaspin 6 mL, Vivascience) [22].

2.2. Bioconjugation protocol of CCMV capsids

As shown in Fig. 1 step (1), CCMV was first modified with an amine by incubating 1 mg/mL CCMV sample (500 μL) with 5 mM propargylamine, aided by 1-ethyl-3-[3-dimethylaminopropyl] carbodiimide hydrochloride (EDC) and N-hydroxysulfosuccinimide sodium salt (sulfo-NHS) in the assembly buffer for 24 h at 4°C. The CCMV-alkyne product was isolated by cesium chloride gradient ultracentrifugation and resuspended in 80% assembly buffer and 20% DMSO. After the optimization and setup of the CuAAC reaction, the conjugation (step (2) in Fig. 1) of CCMV-alkyne with the grafted moieties was performed by incubating 1 mg/mL CCMV-alkyne with 7-(diethylamino) coumarin-3-carbonyl azide, OEG bisazide, and azide-terminated RGD oligopeptide separately, in the presence of 1 mM copper sulfate, 2 mM tris(2-carboxyethyl)phosphine hydrochloride (TCEP), and 3 mM ligand bathocuproin-disulfonic acid disodium salt (BCDS) for 24 h at 4°C.

The corresponding products (coumarin-CCMV, OEG-CCMV, and RGD-CCMV) were purified by two successive series of cesium chloride gradient ultracentrifugation and resuspended in the assembly buffer [22]. The reactions were analyzed by size-exclusion fast protein liquid chromatography (FPLC), sodium dodecyl sulfate polyacrylamide gel electrophoresis (SDS-PAGE), transmission electron microscopy (TEM), dynamic light scattering (DLS), and fluorescence spectroscopy. FPLC was performed on a Biologic DuoFlow™ Chromatography System (Bio-Rad, USA) equipped with a Superose 6 PC 3.2/30 column (Amersham Biosciences). The injection volume was 100 μL, the elution buffer was composed of 50 mM sodium acetate, 500 mM NaCl, and 1 mM DTT at pH 5.0, and the running flow rate was 40 μL/min. TEM images of the sample (5 μL) which was stained with uranyl acetate (5 μL, 2 % w/v) on Formvar-carbon coated grids were obtained with a CM30 electron microscope (FEI/Philips) operated at 200 kV. DLS was employed to measure the hydrodynamic diameters of the nanoparticles formed at physiological pH (Malvern Zetasizer Nano ZS spectrometer). The particle-size distribution of the scattering data was best fit using the Contin algorithm with the average of at least five measurements. Fluorescently labeled CCMV was visualized with an ImageQuant 300 imager (GE Healthcare) before Coomassie blue staining.

2.3. Immobilization of the modified CCMV capsids onto the APTES slides

The modified CCMV capsids (0.5 mg/mL) were adsorbed onto the APTES slides separately. Wild-type CCMV (wt-CCMV) and coumarin-CCMV were used as controls. First, 500 μL virus solutions were dropped onto the substrates (10×10 mm^2) so that they fully covered the surface, and the samples were kept at room temperature in a biosafe hood for 10 min. The samples were washed in pure water and dried at room temperature. The resultant systems were denoted as APTES-coumarin-CCMV, APTES-OEG-CCMV, and APTES-RGD-CCMV, respectively. The adsorbed viral particles onto the APTES slides were prepared for further utilization.

2.4. Cell adhesion with HeLa cells

HeLa cells were cultured in complete Dulbecco's modified Eagles medium (DMEM) supplemented with 10% heat-inactivated fetal calf serum (FCS), 2 mM L-glutamine, 50 μg/mL penicillin and 50 μg/mL streptomycin at 37°C in a humidified 5% CO_2 incubator. Monolayers of HeLa cells in their growth phase (ca. a density of 2×10^4 cells/mL) were routinely split 1:5 in 10 cm culture dishes, placed at 37°C for 5 ~ 10 min, and washed twice in preheated phosphate-buffered saline containing 0.25% (w/v) trypsin-EDTA. After the cells were detached from the dishes, 1 mL preheated DMEM was added, and the cells were transferred into a 50-mL Falcon tube. The cells were spun down and plated in new dishes with fresh culture medium for subsequent binding studies with the APTES-coumarin-CCMV, APTES-OEG-CCMV, and APTES-RGD-CCMV slides. The slides were incubated at 37°C with 5% CO_2 + 95% atmosphere. Cell adhesion, spreading, and proliferation were examined at 5 and 24 h postseeding. Nonadherent cells on the slides were removed by washing with phosphate-buffered saline, and the adherent cells were fixed using formaldehyde and stained with Giemsa stain. Photomicrographs of the cytoplasmic-stained cells were obtained (100 × total magnification using a Nikon Eclipse TS100 microscope). The statistical analysis was performed using a two-tailed unpaired Student's *t*-test ($p < 0.05$).

3. Results and Discussion

3.1. Installation of the alkyne group on the CCMV capsids

As reported, the carboxyl residues of various viral capsids are amenable to reaction with primary amines under activation [23,24]. Therefore, carboxylic groups were chosen for derivatization with alkynes in this study. The reactivity of the CCMV carboxyl groups was tested with fluorescein cadaverine under activation with EDC and sulfo-NHS, which revealed that 560 carboxylates were

modified in high yields [12]. This was approximately 4.7 ~ 6.2 times higher than that accessible in TYMV (90 ~ 120 carboxylic groups) [21]. To explore the potential of introducing a multifunctional group onto the surface of CCMV, the viral capsids were labeled with acetylene at surface-exposed carboxylic groups. More than 90% of the coat protein was recovered by ultracentrifugation after the removal of the small molecules. The high recovery yield encouraged the continuation of the CuAAC reaction between CCMV-alkyne and azides.

3.2. CuAAC reaction on the CCMV-alkyne capsids

The conditions of the CuAAC reaction are crucial for the productivity. $CuSO_4$-sodium ascorbate is the preferred reducing agent for most reactions. However, the byproduct of ascorbate to dehydroascorbate can hydrolyze to form reactive aldehydes, such as 2,3-diketogulonate and presumably glyoxal [25]. These species can react with the arginine, cysteine, and lysine residues on the viral capsid, which subsequently leads to aggregation-dependent decomposition. This was clearly observed in the case of CCMV modification (data not shown). Thus, TCEP and BCDS were introduced for the CuAAC bioconjugations as the Cu(I) source.

The fluorochrome 7-(diethylamino)coumarin-3-carbonyl azide was first employed as the azido counterpart in the CuAAC reaction, which could be easily monitored by the increase in the fluorescence at 475 nm upon formation of a triazole ring [26]. The purified and diluted cycloaddition product coumarin-CCMV produced a strong, detectable fluorescent signal at 475 nm upon excitation at 340 nm. The FPLC results showed that the CCMV particles were stable throughout the click reaction conditions and remained in the assembled state, as indicated by similar elution with the wt-CCMV particles. From Fig. 2, there was a single intact peak at t = 38 min that was similar to that of wt-CCMV, indicating the integrity of the particles and the successful attachment of the coumarin dye. The coumarin-CCMV sample was also analyzed using SDS-PAGE with fluorescence visualization of the attached coumarin, followed by Coomassie blue staining; the results revealed one dye-labeled band corresponding to the same molecular weight of CCMV CP subunit because of the covalent attachment with coumarin (Fig. 3). The TEM image in Fig. 4A confirmed the integrity of the particle after two-step modification, with a size of approximately 30 nm.

Following the same procedure, OEG bisazide and the azide-terminated RGD oligopeptide were also installed onto acetylene-functionalized CCMV. As expected from the high coupling efficiency of the CuAAC reaction, the modified OEG-CCMV and RGD-CCMV were confirmed by FPLC analysis with a similar elution time to that of wt-CCMV particles, indicated by a single intact peak at t = 38 min, verifying the integrity of the particles with OEG attachment (Fig. 2). The TEM images of OEG-CCMV in Figs. 4B and 4C showed a unique phenomenon of connected bridges with the intact capsids crosslinked to each other. As the sticky solution obtained distinguished it from the other samples, a reasonable explanation might stem from the possible double CuAAC reaction from the bisazide. As

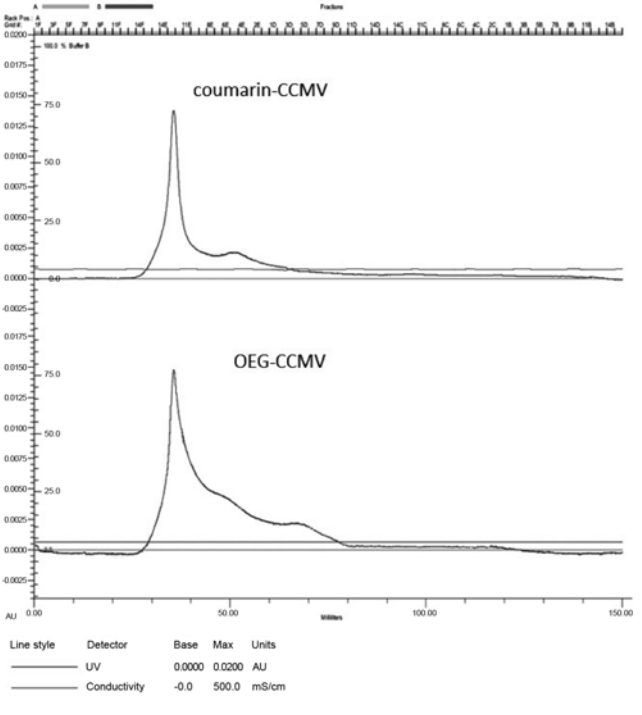

Fig. 2. Size-exclusion FPLC of coumarin-CCMV and OEG-CCMV. The upper curve and lower curve showed a single intact peak at t = 38 min, which was similar to that of wild-type CCMV, indicating the integrity of the particles.

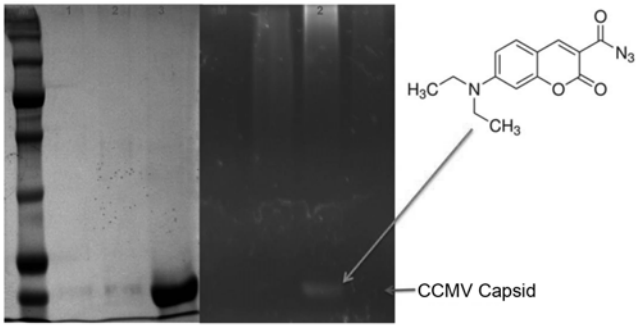

Fig. 3. SDS-PAGE of coumarin-CCMV visualized under UV irradiation and upon Coomassie blue staining. The left was taken under white light after Coomassie blue staining and the right was taken under UV irradiation. Lane 1, alkyne-CCMV; 2, coumarin-CCMV; and 3, wild type CCMV; M, DokDo-MARK^{TM} broad-range.

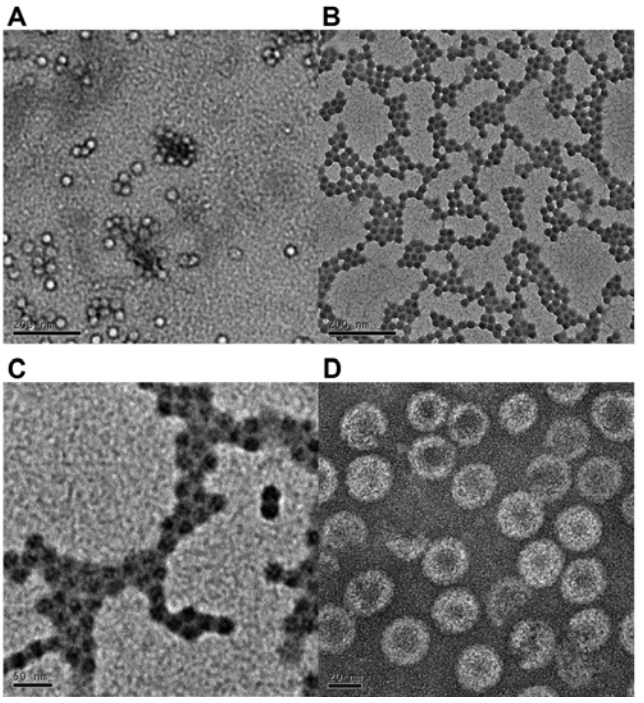

Fig. 4. TEM image of coumarin-CCMV and OEG-CCMV particles. (A) coumarin-CCMV; (B) OEG-CCMV, size bar represents 200 nm; (C) amplified OEG-CCMV, size bar represents 50 nm; (D) wild-type CCMV, size bar represents 20 nm.

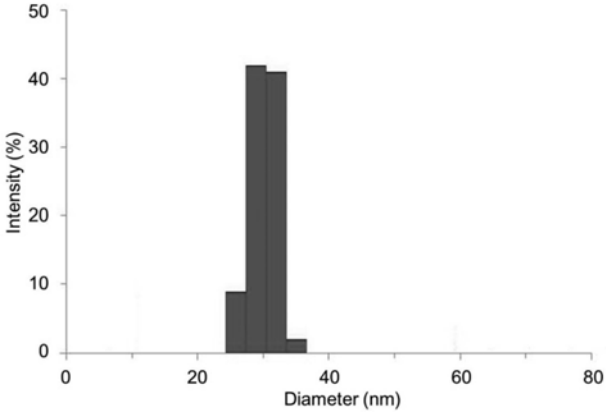

Fig. 5. DLS size distribution of OEG-CCMV particles.

presented in Fig. 5, the hydrodynamic diameter (measured by DLS) for OEG-CCMV was 30.7 ± 1.5 nm.

3.3. Immobilization of modified CCMV capsids on APTES slides

APTES slides were used to immobilize virus particles onto the 2D surfaces prior to the cell-binding studies. APTES is positively charged and can hold negatively charged virus particles on the slides *via* electrostatic interactions under approximately neutral conditions [27,28]. CCMV and

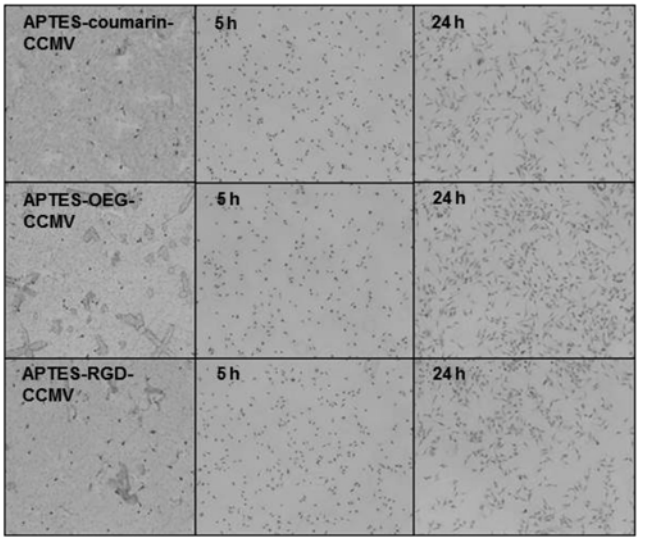

Fig. 6. Optical microscopy of cell adhesion results by different CCMV particles with HeLa cells. (A) APTES-coumarin-CCMV of time 0, 5, and 24 h; (B) APTES-OEG-CCMV of time 0, 5, and 24 h; (C) APTES-RGD-CCMV of time 0, 5, and 24 h.

modified CCMV display negative surface charges at pH 5.2 (pI_{CCMV} ~ 3.6) [29]. First, 500 μL of the modified CCMV capsids (0.5 mg/mL) were adsorbed onto the APTES slides to fully cover the surface, and the samples were then kept at room temperature in a biosafe hood for 10 min. The samples were washed in pure water and dried at room temperature. The adsorbed APTES-coumarin-CCMV, APTES-OEG-CCMV, and APTES-RGD-CCMV slides were put into 12-well plates; 1 mL of HeLa cell suspension in DMEM at a density of 2×10^4 cells/mL was added to each well of the 12-well plate, and the cells were incubated at 37°C in a humidified 5% CO_2 incubator.

3.4. Cell adhesion with HeLa cells

HeLa cells were selected for the preliminary adhesion studies onto the virus-coated silane surface because this cell type has been widely used as a prototype cell to study cell-substrate interactions. RGD tripeptide is a common cell-recognition site of many adhesive proteins contained in the extracellular matrices and in the blood and can bind to integrin receptors of mammalian cells [30,31]. Identified as a pervasive cell-adhesive peptide, RGD has been extensively investigated to enhance the binding activity with mammalian cells [32]. In contrast, OEG presents inhibition to cell binding similar to that of PEG, a water-soluble polymer.

The proliferation and adhesion of HeLa cells with modified CCMV particles were monitored by microscopy after 5 and 24 h post seeding. As shown in Fig. 6, the cell proliferation was verified on all slides. At 5 h, the cell

adhesion of the APTES-OEG-CCMV slides decreased slightly to 77.3% compared to the value of the control APTES-coumarin-CCMV, whereas APTES-RGD-CCMV enhanced the binding by 1.09-fold. This result was similar to those of previous reports [33,34], which demonstrated that, APTES-OEG-CCMV is normally nonadhesive to HeLa cells due to the lack of a biological recognition motif on OEG and its resistance to the binding membrane proteins. However, as time proceeded to 24 h, the HeLa cells on the APTES-OEG-CCMV slides proliferated 1.21-fold compared to those on the control slides; this might be caused by the crosslinked structure of OEG-CCMV. The explanation might depend on the fact that the structure of the OEG polymer with diazide moieties at both termini resulted in a crosslinked structure among the CCMV capsids bridged by triazole ligands, which could further affect the cell-binding process. This unique structure of the modified capsids generated a net-like, sticky solution, which then resulted in higher adhesion with HeLa cells over time. Similar phenomena were reported by Kaur *et al.* [35] using a dialkyne dye molecule for the CuAAC reaction to modify TYMV capsids, which changed the hydrophobicity of the modified capsids at the interface of the two liquids.

Regarding the results of APTES-RGD-CCMV, there was an obvious enhancement in the binding compared with that of the control of APTES-coumarin-CCMV at 5 and 24 h, with a similar increment rate (1.09- and 1.07-fold, respectively). This result indicated that the cell attachment occurred specifically in the existence of the RGD motif on the CCMV capsids, which could provide a more biomimetically suitable and flexible environment for the cells. Additionally, the RGD ligand density and its spatial arrangement could play a significant role during the binding process [36]. Another difference from previously reported results [21,28] was that the HeLa cells did not present similar elongated or stretched morphologies to those of NIH3T3 fibroblasts on APTES slides. This might be attributable to the different properties of these two cell types and their interactions with the APTES ligand on the slides.

4. Conclusion

CCMV capsids were grafted with various moieties from fluorogenic coumarin and OEG short chain to RGD peptides *via* the CuAAC "click" reaction. The carboxyl residues on the exterior surface were chosen to be modified with an alkyne and further modified with an azide by a triazole connection. The CCMV capsids decorated with OEG and RGD showed opposite effects on the cell-adhesion and cell-proliferation behavior.

Compared with other surface-modification methods, ligation utilizing the CuAAC reaction offers a convenient, rapid, and versatile method that is applicable to a wide variety of biomolecules, scaffolds, and cellular components, both *in vitro* and *in vivo*. The modified CCMV capsids have potential applications in bioimaging, tissue engineering, and drug delivery.

Acknowledgements

This work was supported by the research fund from Chosun University, 2013. The authors wish to thank Dr. Soo-Kyung Choi (Chosun University) for providing the TEM images.

Nomenclature

APTES	: 3-aminopropyl-triethoxysilane
BCDS	: Bathocuproindisulfonic acid disodium salt
CCMV	: Cowpea chlorotic mottle virus
CP	: Coat protein
CPMV	: Cowpea mottle virus
CuAAC	: Copper(I)-catalyzed azide-alkyne cycloaddition
DLS	: Dynamic light scattering
DMEM	: Dulbecco's modified Eagles medium
DMSO	: Dimethyl sulfoxide
EDC	: 1-ethyl-3-[3-dimethylaminopropyl] carbodiimide hydrochloride
FCS	: Fetal calf serum
FPLC	: Fast protein liquid chromatography
OEG	: Oligo-ethylene glycol
RGD	: Arg-Gly-Asp
sulfo-NHS	: N-hydroxysulfosuccinimide sodium salt
TCEP	: Tris(2-carboxyethyl)phosphine hydrochloride
TEM	: Transmission electron microscopy
TMV	: Tobacco mosaic virus
TYMV	: Turnip yellow mosaic virus
VLPs	: Virus-like particles

References

1. Liu, Z., J. Qiao, Z. Niu, and Q. Wang (2012) Natural supramolecular building blocks: From virus coat proteins to viral nanoparticles. *Chem. Soc. Rev.* 41: 6178-6194.
2. Bronstein, L. M. (2011) Virus-based nanoparticles with inorganic cargo: What does the future hold? *Small* 7: 1609-1618.
3. Strable, E. and M. G. Finn (2009) Chemical modification of viruses and virus-like particles. *Curr. Top. Microbiol. Immunol.* 327: 1-21.

4. Hosseinkhani, H., W. He, C. Chiang, P. D. Hong, D. S. Yu, A. J. Domb, and K. Ou (2013) Biodegradable nanoparticles for gene therapy technology. *J. Nanopart. Res.* 15: 1-15.
5. Bancroft, J. B., G. J. Hills, and R. Markham (1967) A study of the self-assembly process in a small spherical virus. Formation of organized structures from protein subunits *in vitro*. *Virol.* 31: 354-379.
6. Chen, Z., C. Stauffacher, and J. E. Johnson (1990) Capsid structure and RNA packaging in comovirus. *Semin. Virol.* 1: 453-466.
7. Speir, J. A., S. Munshi, G. Wang, T. S. Baker, and J. E. Johnson (1995) Structures of the native and swollen forms of cowpea chlorotic mottle virus determined by X-ray crystallography and cryo-electron microscopy. *Structure* 3: 63-78.
8. Lee, L. A., Z. Niu, and Q. Wang (2009) Viruses and virus-like protein assemblies--chemically programmable nanoscale building blocks. *Nano Res.* 2: 349-364.
9. Wu, Y., H. Yang, and H. J. Shin (2013) Viruses as self-assembled nanocontainers for encapsulation of functional cargoes. *Kor. J. Chem. Eng.* 30: 1359-1367.
10. Johnson, J. E. and J. A. Speir (1997) Quasi-equivalent viruses: a paradigm for protein assemblies. *J. Mol. Biol.* 269: 665-675.
11. Reddy, V. S., P. Natarajan, B. Okerberg, K. Li, K. V. Damodaran, R. T. Morton, C. L. 3rd Brooks, and J. E. Johnson (2001) Virus Particle Explorer (VIPER), a website for virus capsid structures and their computational analyses. *J. Virol.* 75: 11943-11947.
12. Gillitzer, E., D. Willits, M. Young, and T. Douglas (2002) Chemical modification of a viral cage for multivalent presentation. *Chem. Commun.* 20: 2390-2391.
13. Koudelka, K. J. and M. Manchester (2010) Chemically modified viruses: Principles and applications. *Curr. Opin. Chem. Biol.* 14: 810-817.
14. Kolb, H. C., M. G. Finn, and K. B. Sharpless (2001) Click chemistry: Diverse chemical function from a few good reactions. *Angew. Chem. Int. Ed.* 40: 2004-2021.
15. Rostovtsev, V. V., L. G. Green, V. V. Fokin, and K. B. Sharpless (2002) A stepwise huisgen cycloaddition process: copper(I)-catalyzed regioselective "ligation" of azides and terminal alkynes. *Angew. Chem. Int. Ed.* 41: 2596-2599.
16. Tornøe, C. W., C. Christensen, and M. Meldal (2002) Peptidotriazoles on solid phase: [1,2,3]-triazoles by regiospecific copper(i)-catalyzed 1,3-dipolar cycloadditions of terminal alkynes to azides. *J. Org. Chem.* 67: 3057-3064.
17. Hong, V., S. I. Presolski, C. Ma, and M. G. Finn (2009) Analysis and optimization of copper-catalyzed azide-alkyne cycloaddition for bioconjugation. *Angew. Chem. Int. Ed.* 48: 9879-9883.
18. Wang, Q., T. R. Chan, R. Hilgraf, V. V. Fokin, K. B. Sharpless, and M. G. Finn (2003) Bioconjugation by copper(I)-catalyzed azide-alkyne [3 + 2] cycloaddition. *J. Am. Chem. Soc.* 125: 3192-3193.
19. Gupta, S. S., J. Kuzelka, P. Singh, W. G. Lewis, M. Manchester, and M. G. Finn (2005) Accelerated bioorthogonal cojugation: A practical method for ligation of diverse functional molecules to a polyvalent virus scaffold. *Bioconjugate Chem.* 16: 1572-1579.
20. Bruckman, M. A., G. Kaur, L. A. Lee, F. Xie, J. Sepulveda, R. Breitenkamp, X. Zhang, M. Joralemon, T. P. Russell, T. Emrick, and Q. Wang (2008) Surface modification of tobacco mosaic virus with "Click" chemistry. *ChemBioChem* 9: 519-523.
21. Zeng, Q., S. Saha, L. A. Lee, H. Barnhill, J. Oxsher, T. Dreher, and Q. Wang (2011) Chemoselective modification of turnip yellow mosaic virus by Cu(I) catalyzed azide–alkyne 1,3-dipolar cycloaddition reaction and its application in cell binding. *Bioconjugate Chem.* 22: 58-66.
22. Wu, Y., H. Yang, and H. J. Shin (2014) Encapsulation and crystallization of Prussian blue nanoparticles by cowpea chlorotic mottle virus capsids. *Biotechnol. Lett.* 36: 515-521.
23. Schlick, T. L., Z. Ding, E. W. Kovacs, and M. B. Francis (2005) Dual-surface modification of the tobacco mosaic virus. *J. Am. Chem. Soc.* 127: 3718-3723.
24. Steinmetz, N. F., G. P. Lomonossoff, and D. J. Evans (2006) Cowpea mosaic virus for material fabrication: Addressable carboxylate groups on a programmable nanoscaffold. *Langmuir* 22: 3488-3490.
25. Shangari, N., T. S. Chan, K. Chan, S. H. Wu, and P. J. O'Brien (2007) Copper-catalyzed ascorbate oxidation results in glyoxal/AGE formation and cytotoxicity. *Mol. Nutr. Food Res.* 51: 445-455.
26. Sivakumar, K., F. Xie, B. M. Cash, S. Long, H. N. Barnhill, and Q. Wang (2004) A fluorogenic 1,3-dipolar cycloaddition reaction of 3-azidocoumarins and acetylenes. *Org. Lett.* 6: 4603-4606.
27. Yamada, K., S. Yoshii, S. Kumagai, I. Fujiwara, K. Nishio, M. Okuda, N. Matsukawa, and I. Yamashita (2006) High-density and highly surface selective adsorption of protein-nanoparticle complexes by controlling electrostatic interaction. *Jpn. J. Appl. Phys.* 45: 4259-4264.
28. Rong, J., L. A. Lee, K. Li, B. Harp, C. M. Mello, Z. Niu, and Q. Wang (2008) Oriented cell growth on self-assembled bacteriophage M13 thin films. *Chem. Commun.* 41: 5185-5187.
29. Lavelle, L., M. Gingery, M. Phillips, W. M. Gelbart, C. M. Knobler, R. D. Cadena-Nava, and J. Ruiz-Garcia (2009) Phase diagram of self-assembled viral capsid protein polymorphs. *J. Phys. Chem. B.* 113: 3813-3819.
30. Waldeck, J., F. Häger, C. Höltke, C. Lanckohr, A. von Wallbrunn, G. Torsello, W. Heindel, G. Theilmeier, M. Schäfers, and C. Bremer (2008) Fluorescence reflectance imaging of macrophage-rich atherosclerotic plaques using an alphav-beta3 integrin-targeted fluorochrome. *J. Nucl. Med.* 49: 1845-1851.
31. Laitinen, I., A. Saraste, E. Weidl, T. Poethko, A. W. Weber, S. G. Nekolla, P. Leppänen, S. Ylä-Herttuala, G. Hölzlwimmer, A. Walch, I. Esposito, H. J. Wester, J. Knuuti, and M. Schwaiger (2009) Evaluation of alphavbeta3 integrin-targeted positron emission tomography tracer 18F-galacto-RGD or imaging of vascular inflammation in atherosclerotic mice. *Circ. Cardiovasc. Imaging* 2: 331-338.
32. Flores, K. A., J. C. Salgado, G. Zapata-Torres, Z. P. Gerdtzen, M. J. Gonzalez, and M. A. Hermoso (2012) Effect of the electrostatic potential on the internalization mechanism of cell penetrating peptides derived from TIRAP. *Biotechnol. Bioproc. Eng.* 17: 485-499.
33. Desai, N. P. and J. A. Hubbell (1991) Biological responses to polyethylene oxide modified polyethylene terephthalate surfaces. *J. Biomed. Mater. Res.* 25: 829-843.
34. McPherson, T., A. Kidane, I. Szleifer, and K. Park (1998) Prevention of protein adsorption by tethered poly (ethylene oxide) layers: Experiments and single-chain mean-field analysis. *Langmuir* 14: 176-186.
35. Kaur, G., W. Zhan, C. Wang, H. Barnhill, H. Tian, and Q. Wang (2010) Crosslinking of viral nanoparticles with "clickable" fluorescent crosslinkers at the interface. *Sci. China Chem.* 53: 1287-1293.
36. Rhee, S. and F. Grinnell (2007) Fibroblast mechanics in 3D collagen matrices. *Adv. Drug Delivery Rev.* 59: 1299-1305.